Journal Name

ARTICLE

A comparison of copper and acid site zeolites for the production of nitric oxide for biomedical applications

Samantha E. Russell,[a] Juan María González Carballo,[b] Claudia Orellana-Tavra,[c] David Fairen-Jimenez[c] and Russell E. Morris[a]

Copper-exchanged and acidic zeolites are shown to produce nitric oxide (NO) from a nitrite source in biologically active (nanomolar) concentrations. Four zeolites were studied; mordenite, ferrierite, ZSM-5 and SSZ-13, which had varying pore size, channel systems and Si/Al ratios. ZSM-5 and SSZ-13 produced the highest amounts of NO in both the copper and acid form. The high activity and regeneration of the copper active sites makes them good candidates for long-term NO production. Initial cytotoxicity tests have shown at least one of the copper zeolites (Cu-SSZ-13) to be biocompatible, highlighting the potential usage within biomedical applications.

Introduction

The discussion of zeolites and nitric oxide (NO) most frequently relates to de-NOx catalysis, where zeolites work to reduce NO emissions at high temperatures in car exhausts.[1–3] Here we discuss an interesting manipulation of this well-known process with zeolites that can produce NO at room temperatures. NO is an extremely important molecule within the body, with the discovery of its signalling properties awarded a Nobel Prize in 1998. Materials that deliver this molecule therefore have potential to be used in medical applications due to the anti-thrombotic and vasodilating properties of NO.[4–6]

Up until now, the vast majority of NO delivery mechanisms have involved NO stored inside the materials and delivered when required. Porous materials, such as MOFs and zeolites, have been used for NO storage and release, where upon exposure to water the NO molecules are displaced, delivering the gas.[7,8] Other methods have used NO donor molecules, where compounds such as sodium nitroprusside (SNP) and glyceryl trinitrate (GTN), decompose within the body to release NO.[9] Both methods have shown to be very effective for a range of ailments, such as wound-healing,[10] rapid blood pressure lowering[11] and pain relief for angina.[12] The obvious disadvantage of stored NO is that the reservoir will eventually run out at some point, making stored NO suitable only for relatively short-term applications. However, there are several examples of the chemical production of NO. Perhaps the most important of these is the use of the nitrite ion as a substrate from which NO is produced. This can be done in two ways, either by the reaction of nitrite with an acid[13] or by interaction of nitrite with copper ions.[14] The acidified nitrite route is one that has received much attention, but one potential drawback is that this chemical route has been shown to produce severe inflammatory response in certain situations.[15] This response has been ascribed to side products of the reaction. Copper-mediated production of NO has also been studied as a potential source of biomedically active NO,[16] with copper ions being accommodated within polymers[17] and porous materials, including examples of metal-organic frameworks,[18] mesoporous materials[19] and a copper zeolite.[20] The significant advantage of this type of approach over stored NO approaches is that there is the possibility of replenishing the source of the nitrite substrate for as long as the activity of the material remains potent enough. There is also the advantage that materials that store NO may need to be stored under special conditions (e.g. away from moisture). Such requirements should not be necessary for acid- or copper-mediated production of NO. Here we compare four well-known zeolite materials (mordenite, ferrierite, ZSM-5 and SSZ-13) in the acid and copper-exchanged form for the production of nitric oxide from biologically available sources. Cysteine and nitrite are both abundant within blood plasma, with concentrations of 250 µmol/L and 4.2 µmol/L, respectively.[21,22] While the nitrite acts as a substrate for both active sites, the cysteine works as a sacrificial reductant to generate the active copper site, **Figure 1**. All four zeolites have been heavily studied for their deNOx potential, and Cu-SSZ-13 has, in particular, been a recent addition to commercially-used zeolites in automotive deNOx applications. This material has excellent properties for the destruction of NO, but it should also have good properties for NO production – small pores to aid selectivity towards small

a. School of Chemistry, University of St. Andrews, Purdie Building, St. Andrews KY16 9ST, UK
b. Sasol UK Ltd, Purdie Building, St Andrews KY16 9ST, UK
c. Department of Chemical Engineering & Biotechnology, University of Cambridge, Cambridge CB2 3RA, UK
d. † Footnotes relating to the title and/or authors should appear here.
Electronic Supplementary Information (ESI) available: [details of any supplementary information available should be included here]. See DOI: 10.1039/x0xx00000x
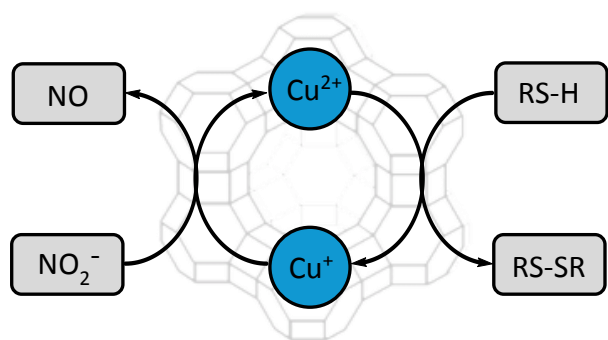
Figure 1: The catalytic cycle of copper within the pores of the zeolite upon the addition of a sacrificial reductant. The cysteine hydrochloride (RS-H) reduces Cu^{2+} to Cu^+, resulting in the formation of an active copper species and an oxidised disulfide bridging cystine molecule. The active Cu^+ then reacts with a nitrite molecule, producing NO, resulting in the oxidation of Cu^+ back to Cu^{2+}.

products like NO (and so limit any possible side products), good hydrothermal stability etc. Our hypothesis was therefore that SSZ-13 should be an excellent material to produce NO from nitrite.

Experimental

Zeolite Syntheses

Ferrierite was synthesised according to the standard literature for zeolite synthesis[23] with a batch composition of 1.85 Na_2O : Al_2O_3 : 15.2 SiO_2 : 592 H_2O : 19.7 ethylenediamine. The copper-exchanged mordenite sample was synthesised from literature[24] with a batch composition of 12 Na_2O : 2Al_2O_3 : 100 SiO_2 : 500 H_2O. The acidic mordenite sample was also synthesised from literature[23] with a batch composition of 6 Na_2O : Al_2O_3 : 30 SiO_2 : 780 H_2O. NH_4-ZSM-5 was obtained from Zeolyst (CBV 3024E) and H-SSZ-13 was obtained from Chevron. Full synthesis details can be found in the SI. The purity of the synthesised samples were determined by powder X-ray diffraction (PXRD), and their morphologies studied by scanning electron microscopy (SEM), **Figure S1** and **S2** respectively. PXRD samples were run on a PANalytical Empyrean, Cu X-ray tube, primary beam monochromator (CuKa1), 15-position sample changer with an X'celerator RTMS detector. SEM samples were gold coated by a Quorum Q150R ES coating system and images recorded with a Jeol JSM-5600 Scanning Electron Microscope with an Oxford Inca EDX system.

Active Site Formation

The Brønsted acid sites of each zeolite were formed by ion-exchanging the zeolites with ammonium cations using ammonium chloride solution (0.3 M), followed by calcination at high temperature. Ammonium chloride solution and zeolite (10 mL/50 mg) were stirred overnight at room temperature. The solid was then filtered and washed. This exchange procedure was repeated three times. The ion-exchanged

sample was then calcined at 575 °C for 6 hours at a rate of 1.5 °C /min to release ammonia, forming the acid site. The number and strength of the sites were studied using ammonia temperature programmed desorption (NH_3-TPD).

The copper sites were formed by copper ion-exchange. The zeolites were stirred with copper nitrate solution (0.3 M) for up to 24 hours at 90 °C using 10 mL/50 mg zeolite. The exchanged sample was then filtered and washed with water. The exchange efficiency was studied using energy dispersive X-ray spectroscopy (EDX), with a target Cu/Al ratio of approximately 0.5. It is assumed that the nitrate anions form sodium nitrate with the sodium cations that are exchanged out of the zeolite pores. The sodium nitrate will remain in solution and be removed upon filtration.

Ammonia Temperature Programmed Desorption (NH_3-TPD)

The strength and number of acid sites in the acid zeolites were studied by NH_3-TPD using a Micromeritics AutoChem 2950 coupled to a Balzers Thermostar quadrupole Mass Spectrometer. 80 mg of the zeolite samples were loaded into the U-shaped quartz reactor. Firstly, each sample was dehydrated following a two stage process by heating at 120 °C for 30 minutes, and then at 500 °C for 20 minutes under Ar. The system was then cooled down to 100 °C and the flow switched to ammonia (15 volume % NH_3 in He) flow for 60 minutes. The reactor was then evacuated with argon gas for 60 minutes to remove any free, unbound ammonia molecules. The bound ammonia was finally desorbed from the zeolites with a gradual temperature increase from 100 °C to 500 °C with a heating ramp of 10 °C/min. Ammonia desorption was monitored by mass spectrometry (m/z 17).

NO Production Testing

The activities of the zeolites were studied by the conversion of sodium nitrite to nitric oxide. 5 mg of zeolite and 2.6 mL of distilled water were stirred in a capped vial, with a nitrogen gas inlet. The NO produced after an injection of sodium nitrite was carried to a Sievers 280i Nitric Oxide Analyser (NOA) via an outlet needle. The NOA monitored the concentration of NO produced throughout the reaction, allowing determination of total NO production. All runs were recorded in triplicate.

Cysteine hydrochloride (0.05 M, 25 µL) was injected 5 minutes into the run, followed by a sodium nitrite injection (0.05 M, 5 µL) 15 minutes into the run. The acid sites did not require activation; therefore only sodium nitrite (0.05 M, 250 µL) was required and injected 5 minutes into the run.

Copper Cytotoxicity Testing

The cytotoxicity of the copper zeolites was determined by measuring the cellular metabolic activity using an MTS reduction assay. The viability of HeLa cells was studied after 24 hour incubation with ranging concentrations of copper zeolites (0, 0.25, 0.50 and 1.00 mg/mL). The viability values for the differing concentrations were normalised by the control value of untreated cells (cells incubated only with growth media and no zeolite). Full protocol described in SI.

Results and Discussion

Zeolite Characterisation

EDX was used to determine the final Si/Al of the zeolites. Different synthesis batches of mordenite were used for the copper and acid sites. Mordenite with a Si/Al ratio of 6.00 was used for the copper sites and a Si/Al of 7.76 was used for the acid sites. All other zeolites used the same batch for both the acid and copper sites. Ferrierite had a Si/Al of 6.05, ZSM-5 15.17 and SSZ-13 15.17 also.

Ammonia Temperature Programmed Desorption (NH$_3$-TPD)

Figure 2 shows the m/z 17 profiles monitored during the NH$_3$-TPD. The profiles are governed by two desorption peaks, one in the region of 100 − 275 °C which corresponds to weakly bound NH$_3$ and the second from 275 − 500 °C which corresponds to strongly bound NH$_3$. The second desorption peak correlates to the acid site strength and the number of acid sites. The lowest desorption temperature, and therefore weakest acid, is H-ZSM-5 which peaks around 400 °C. The greatest desorption temperature, and therefore strongest acid, is H-MOR which peaks around 500 °C. The desorption profiles of MOR and FER reveals that temperatures above 500 °C are necessary to fully desorb NH$_3$. This highlights the higher acidity of these materials compared to ZSM-5 and SSZ-13. Due to this, attempts to quantify the number of acid sites by integrating the area under the profile may lead to incorrect data. Therefore, the peak heights suggest currently that H-ZSM-5 has the lowest number of acid sites and H-SSZ-13 has the greatest. Overall we observe acid site strength as MOR>SSZ-13>FER>ZSM-5 and acid site number as SSZ-13>MOR>FER>ZSM-5.

Acid Sites

The average total NO produced by the four acid site zeolites from the triplicate runs is shown in **Figure 3a.**
H-SSZ-13 and H-ZSM-5 produce the highest total amounts of NO, producing 337 nmols and 326 nmols respectively. Their rates of production, however, are quite different; this can be seen by the gradients of the lines in the first couple of hours. H-MOR produces an average of 241 nmols of NO per run making it the next highest production. H-FER has the lowest average production with 187 nmols of NO per run. Similar to the previously discussed difference in rate of production with H-ZSM-5 and H-SSZ-13, the initial rate of NO production for H-FER is higher than that of H-MOR. This may due to pore size or particle size. There was a variation in the length of time that the zeolites produced NO, ranging from around 5 to 8 hours. The general trend of the acid site zeolites was a relatively low initial NO concentration with a long production time.
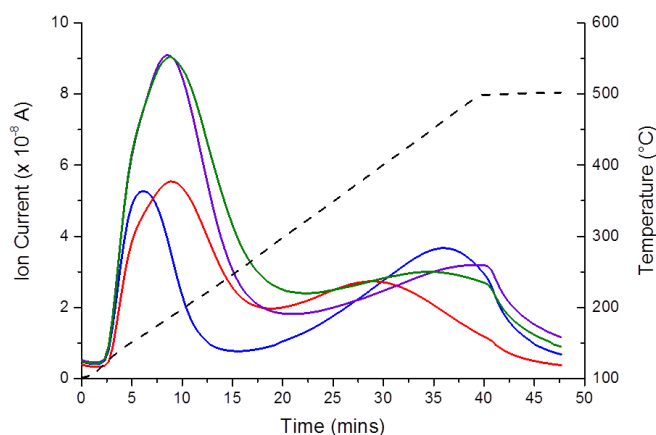

Figure 2: The overlay of the four desorption profiles following m/z of 17, MOR: purple, FER: green, ZSM-5: red and SSZ-13: blue. The high temperature peak provides information on acid strength (peak position) and number of acid sites (peak height). The results show mordenite to have the strongest acid sites and ZSM-5 the weakest. SSZ-13 has the greatest number of acid sites and ZSM-5 the lowest.

Interestingly, there is little obvious correlation between the NH$_3$-TPD results and the amount of NO produced. H-SSZ-13 had the greatest number of acid sites and the second highest strength, therefore the greatest NO production was expected. H-ZSM-5 however, had an extremely similar NO production to H-SSZ-13, yet has the weakest and lowest number of acid sites, while H-MOR was the strongest acid sites, yet had the third lowest production. This suggests that the accessibility of the active sites may be a limitation for mordenite and ferrierite. This would explain why the small pores and 3D channel systems of SSZ-13 and ZSM-5 may favour interaction between the active sites and the nitrite over the larger pored and lower channel systems of mordenite and ferrierite.

Copper Sites

EDX data confirmed that all zeolites had been exchanged to the optimum level with a Cu/Al ratio of approximately 0.5, data shown in **Tables S1 − S4**. The average total NO produced by the four copper site zeolites from the triplicate runs is shown in **Figure 3b.**
The results show Cu-SSZ-13 to have the highest NO production with around 270 nmols of NO produced over a period of roughly 1 hour. The second highest production was from Cu-ZSM-5 which produced around 267 nmol of NO and took around 1.5 hours for total production. Cu-MOR had the third highest production of NO with around 130 nmols produced. This production was considerably longer, lasting around 6 hours, at least 2 hours longer than any other copper zeolite studied. Cu-FER had a total NO production of around 80 nmols produced over a period of around 4 hours.
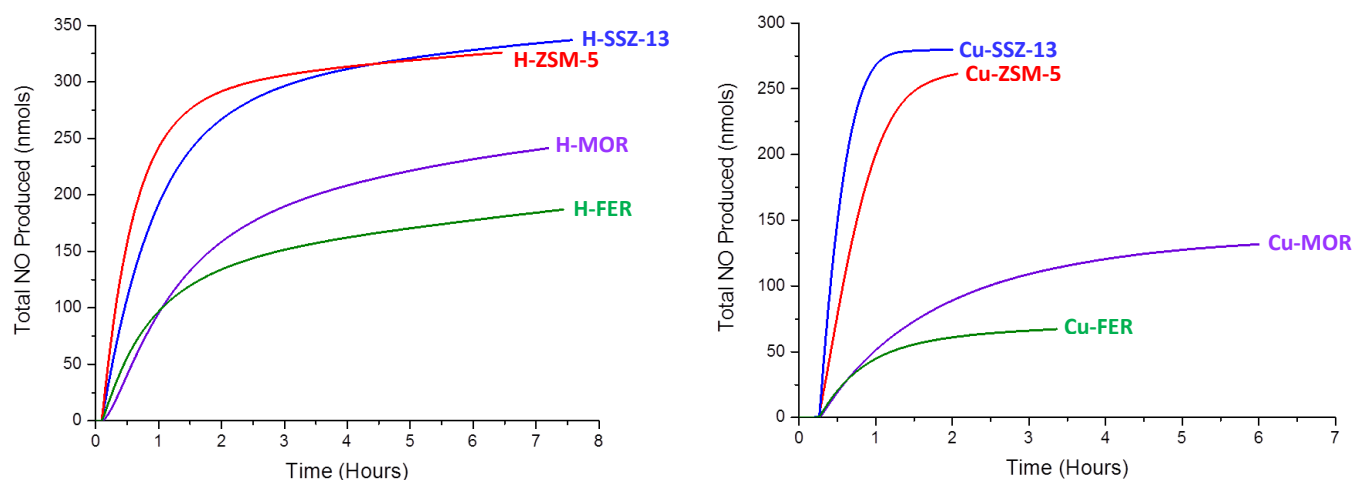
Figure 3a (left): The total NO production for the acid site samples after one injection of sodium nitrite (1.25 x10^{-5} mols) at 5 minutes. **Figure 3b (right)**: The total NO production for the copper site samples after an injection of cysteine hydrochloride (1.25 x10^{-5} mols) at 5 minutes and an injection of sodium nitrite (2.5 x10^{-7} mols) at 15 minutes. The results for both active sites show SSZ-13 and ZSM-5 to have the highest NO production, followed by MOR and finally FER.

The fact that mordenite and ferrierite have higher aluminium contents, and therefore higher copper content, and also larger pores, but still a lower and slower rate of nitrite conversion, suggest the channel system has a great impact on the reactivity. The lower channel systems of mordenite and ferrierite (1D and 2D respectively) indicate that active site accessibility may be limiting the zeolite activity. The small pore, high channel systems (3D) of SSZ-13 and ZSM-5 may favour the interaction of the nitrite with the active sites, as previously observed with the acid sites.

Further studies of the active site location, both before and after the substrate injection, would aid in understanding the difference in activity observed by the four zeolites. Previous work has suggested that the presence and stability of active sites at the channel intersections may explain the difference in catalytic activity of ferrierite and ZSM-5.[25] This may be similar reasoning for why we have observed different activities for the four zeolites, with the same activity order observed with both the copper and acid active sites.

Comparing the two sites, it is apparent that the copper sites are considerably more active than the acid sites, shown by the much lower volume of substrate required to obtain similar concentrations of NO. 250 µL of sodium nitrite was used for the acid sites compared to the 5 µL used for the copper sites, a 50 times increase, highlighting the difference in activity.

Copper Cytotoxicity

The obtained data shows any decrease in cell viability in comparison to normalised cell growth. A drop below 80 % of cell viability was deemed a negative impact on cell growth and therefore cytotoxic. Cu-SSZ-13 was shown to be biocompatible, with cell viability not dropping below 100 % with any zeolite concentration, **Figure 4**. Cu-FER and Cu-ZSM-5 both showed a gradual decrease in cell viability with increasing

zeolite concentration, therefore the use of these materials in biomedical applications would be concentration dependent. Finally, Cu-MOR showed a relatively large drop in cell viability with any concentration of zeolite, showing a low biocompatibility. These results are likely related to the stability of the copper zeolites. Cu-SSZ-13 has been reported to have long term stability over a range of harsh conditions, with the copper addition even increasing stability from the ammonium
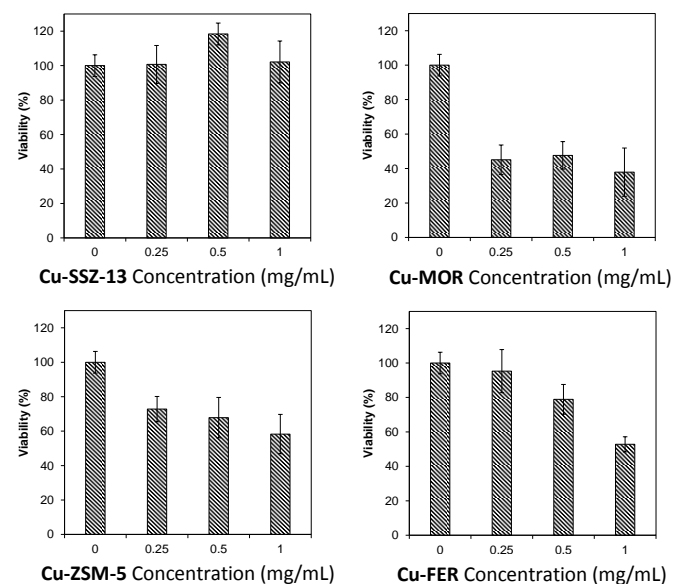

Figure 4: Cytotoxicity tests of the copper zeolites by MTS assay. Results show HeLa cell viability after 24 hour incubation with four concentrations of copper zeolites. Cu-SSZ-13 showed a high biocompatibility with 100 % cell viability continuing after incubation with ranging zeolite concentrations.

exchanged counterpart, therefore highlighting the stability of the structure and explaining the biocompatibility.[26,27]

Active Site Regeneration

Due to the proposed biomedical applications, it is beneficial that the zeolites are able to regenerate the active site to allow a catalytic production and therefore a long-term NO production. Subsequent nitrite injections were performed with both a selected copper and acid site zeolite (Cu-SSZ-13 and H-SSZ-13) to observe if the initial amount of NO produced was obtained from a second substrate injection. An excess of cysteine hydrochloride was initially injected into the copper sample to ensure it was not a limiting factor for the copper sites.

The results in **Figure 5** show that the copper sites of Cu-SSZ-13 do not lose activity after three nitrite injections, with all injections producing between 265 and 282 nmols of NO, as shown by the total NO produced. This suggests that the copper sites are successfully being regenerated through the use of cysteine as a sacrificial reductant. This reveals the high potential for long term NO production. The release profile of a sample of H-SSZ-13 showed that a second injection of substrate produced a considerably lower amount of NO than the first, indicating that the acid site has been consumed during the first reaction with nitrite. The lack of acid site regeneration inhibits their use within long term NO producing applications, such as medical device coatings. Although currently not suitable for long-term NO production, acid site zeolites still have great potential in other areas, such as wound healing, where it may be possible to avoid the previously discussed inflammatory response observed from other routes.

Conclusions

The results reported show the ability of both copper and acid site mordenite, ferrierite, ZSM-5 and SSZ-13 to produce nitric oxide from sodium nitrite. The best performing zeolites were SSZ-13 and ZSM-5, both producing the highest total amounts of NO. The zeolite activity appears to be influenced by the active site location within the pores, therefore future work studying the positions is essential to understand the accessibility of the sites.

The differences between the two active sites are important for considering biomedical applications, with activity and regeneration two key factors. The current inability of the acid sites to be regenerated limits their use in long term NO production, but still have potential in other applications. The copper sites, however, have shown promising results with both high activity and the ability to be regenerated through the use of a sacrificial reductant, highlighting their potential in biomedical applications. Furthermore, toxicology results show the biocompatibility of SSZ-13, indicating great promise for the zeolite use within the body. The biologically active concentrations of NO produced would be suitable for vasodilation and the inhibition of platelet aggregation, therefore being an excellent candidate for biomedical applications.
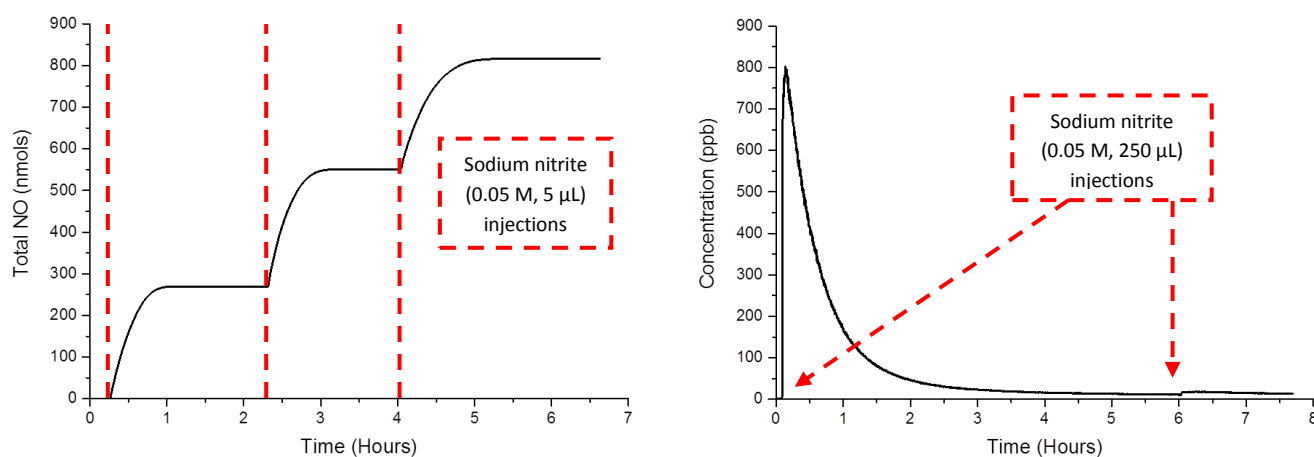

Figure 5 (left): The recyclability of a copper site SSZ-13 sample shown by the total NO produced. After an initial injection of cysteine hydrochloride (0.05 M, 25 µL) at 5 minutes, 3 consecutive sodium nitrite (0.05 M, 5 µL) injections were performed, waiting for complete NO production between each. **Figure 5 (right):** The NO release profile reveals the lack of regeneration of the acid sites, shown by a second substrate injection with significantly less NO produced. This indicates that the acid site is used up in the reaction with nitrite.

Acknowledgements

Notes and references

‡ Footnotes relating to the main text should appear here. These might include comments relevant to but not central to the matter under discussion, limited experimental and spectral data, and crystallographic data.
§
§§

1   H. Yahiro and M. Iwamoto, *Appl. Catal.*, 2001, **222**, 163–181.

2   M. P. Attfield, S. J. Weigel and A. K. Cheetham, *J. Catal.*, 1997, **170**, 227–235.

3   P. Ciambelli, P. Corbo, M. C. Gaudino, F. Migliardini and D. Sannino, *Top. Catal.*, 2001, **16**, 413–417.

4   L. J. Ignarro, G. M. Buga, K. S. Wood and R. E. Byrns, *Sci. York*, 1987, **84**, 9265–9269.

5   D. O. Schairer, J. S. Chouake, J. D. Nosanchuk and A. J. Friedman, *Virulence*, 2012, **3**, 271–9.

6   V. Calabrese, C. Mancuso, M. Calvani, E. Rizzarelli, D. A. Butterfield and A. M. G. Stella, *Nat. Rev. Neurosci.*, 2007, **8**, 766–75.

7   P. S. Wheatley, A. R. Butler, M. S. Crane, S. Fox, B. Xiao, A. G. Rossi, I. L. Megson and R. E. Morris, *J. Am. Chem. Soc.*, 2006, **128**, 502–509.

8   a. C. McKinlay, J. F. Eubank, S. Wuttke, P. S. Wheatley, P. Bazin, J.-C. Lavalley, M. Daturi, A. Vimont, G. De Weireld, P. Horcajada, C. Serre and R. E. Morris, *Chem. Mater.*, 2013, **25**, 1592 – 1599.

9   L. J. Ignarro, C. Napoli and J. Loscalzo, 2011.

10   M. Neidrauer, U. K. Ercan, A. Bhattacharyya, J. Samuels, J. Sedlak, R. Trikha, K. A. Barbee, M. S. Weingarten and S. G. Joshi, *J. Med. Microbiol.*, 2014, **63**, 203–209.

11   S. Das and K. N. Kumar, *Life Sci.*, 1995, **57**, 1547–1556.

12   M. R. Miller and I. L. Megson, *Br. J. Pharmacol.*, 2007, **151**, 305–21.

13   R. Weller, A. D. Ormerod, R. P. Hobson and N. J. Benjamin, *J. Am. Acad. Dermatol.*, 1998, **38**, 559–563.

14   A. Burg, E. Lozinsky, H. Cohen and D. Meyerstein, *Eur. J. Inorg. Chem.*, 2004, 3675–3680.

15   M. Mowbray, X. Tan, P. S. Wheatley, R. E. Morris and R. B. Weller, *J. Invest. Dermatol.*, 2008, **128**, 352–360.

16   M. Kujime and H. Fujii, *Angew. Chemie - Int. Ed.*, 2006, **45**, 1089–1092.

17   B. K. Oh and M. E. Meyerhoff, *Biomaterials*, 2004, **25**, 283–293.

18   J. L. Harding and M. M. Reynolds, *J. Am. Chem. Soc.*, 2012, **134**, 3330 – 3333.

19   A. K. Boës, B. Xiao, I. L. Megson and R. E. Morris, *Top. Catal.*, 2009, **52**, 35–41.

20   A. Boes, P. S. Wheatley, B. Xiao, L. Megson and R. E. Morris, *Chem. Commun.*, 2008, 6146–6148.

21   B. De Chiara, V. Sedda, M. Parolini, J. Campolo, R. De Maria, R. Caruso, G. Pizzi, O. Disoteo, C. Dellanoce, A. R. Corno, G. Cighetti and O. Parodi, *Sci. World J.*, 2012, **303654**.

22   H. Moshage, B. Kok, R. Huizenga and P. L. M. Jansen, *Clin. Chem.*, 1995, **41**, 892–896.

23   H. Robson, in *Syntheses of Zeolitic Materials*, 2001, pp. 1 – 177.

24   H. M. Aly, M. E. Moustafa and E. A. Abdelrahman, *Adv. Powder Technol.*, 2012, **23**, 757–760.

25   P. Nachtigall, M. Davidova and D. Nachtigallova, *J. Phys. Chem. B*, 2001, **105**, 3510–3517.

26   F. Göltl, R. E. Bulo, J. Hafner and P. Sautet, *J. Phys. Chem. Lett.*, 2013, **4**, 2244–2249.

27   D. W. Fickel and R. F. Lobo, *J. Phys. Chem. C*, 2010, **114**, 1633–1640.